Infectious Disease Modelling 8 (2023) 603–616

Contents lists available at ScienceDirect

Infectious Disease Modelling

journal homepage: www.keaipublishing.com/idm

Assessing the efficacy of health countermeasures on arrival time of infectious diseases

Yusuke Asai

Disease Control and Prevention Center, National Center for Global Health and Medicine, 1-21-1 Toyama, Shinjuku-ku, Tokyo, 162-8655, Japan

ARTICLE INFO

Article history:
Received 4 February 2023
Received in revised form 18 April 2023
Accepted 22 May 2023
Available online 26 May 2023
Handling editor: Dr Yijun Lou

Keywords:
Epidemic model
Arrival time
Health countermeasures
Quarantine
Random ODE

ABSTRACT

Public health measures to control the international spread of infectious diseases include strengthening quarantines and sealing borders. Although these measures are effective in delaying the importation of infectious diseases, they also have a significant economic impact by stopping the flow of people and goods. The arrival time of infectious diseases is often used to assess quarantine effectiveness. Although the arrival time is highly dependent on the number of infected cases in the endemic country, direct comparisons have not yet been made. Therefore, this study derives an explicit relationship between the number of infected cases and arrival time. Transmission behavior is stochastic, and deterministic models are not always realistic. In this study, random differential equations, which are differential equations with stochastic processes, were used to describe the dynamics of infection in an endemic country. Furthermore, the flow of travelers from the endemic country was described in terms of survival time, and the arrival time in each country was calculated. A scenario in which PCR kits were distributed between endemic and disease-free countries was also considered, and the impact of different distribution rates on arrival time was evaluated. The simulation results showed that increasing the distribution of PCR kits in the endemic country was more effective in delaying arrival times than using PCR kits in quarantine in disease-free countries. It was also found that increasing the proportion of identified infected persons in the endemic country, leading to isolation, was more important and effective in delaying arrival times than increasing the number of PCR tests.

1. Introduction

The development of airline networks has led to an increase in travel. While the economy has been boosted by active logistics and people, the movement of unwanted goods, such as infectious diseases, has also increased. Since 2000, there have been global outbreaks of infectious diseases, such as Severe Acute Respiratory Syndrome (SARS), Middle East Respiratory Syndrome (MERS), Influenza A (H1N1), and COVID-19. Once an infectious disease is introduced across national borders, it can spread throughout the community and may take a long time to be eradicated. The economic impact is also significant. For example, the

Abbreviations: RODE, Random ordinary differential equation; SDE, Stochastic differential equation.

E-mail address: yuasai@ri.ncgm.go.jp.

Peer review under responsibility of KeAi Communications Co., Ltd.

https://doi.org/10.1016/j.idm.2023.05.004

COVID-19 epidemic, which began in December 2019, infected 754,018,841 people worldwide and caused 6,817,478 deaths as of February 3, 2023, (World Health Organization Coronavirus, 2023). After three years, the epidemic is still not under control, but life is returning to the way it was before COVID-19 because of new knowledge and data, the development and introduction of new drugs and vaccines, and measures such as the introduction of PCR testing and physical distancing.

Public health measures against infectious diseases include personal protective measures at the individual level, such as hand hygiene and use of masks; social measures, such as physical distancing; population-based measures, such as home and school closures, vaccination, and large-scale PCR testing; and city- and country-level measures, such as lockdowns, travel restrictions, and enhanced quarantine (Brümmer et al., 2021; Chu et al., 2020; Mina & Andersen, 2021; Rosella et al., 2022; Talic et al., 2021). Among these, quarantine is one of the measures implemented to prevent the introduction of infectious diseases into a country and to safeguard humans as well as animals and plants. On the other hand, the existence of asymptomatic cases and incubation periods prevent quarantine from being 100% effective in preventing the introduction of infectious diseases. Therefore, even if quarantines are strengthened, the possibility of the infection spreading in the city through asymptomatic cases, and escaping quarantine, cannot be ruled out. Nonetheless, quarantines are expected to have a delaying effect on the importation of the disease. Quarantine is used in many countries during epidemics, as it is expected to have the secondary effect of buying time until infectious diseases are imported, and during this time, the medical system can be improved to prepare for the epidemic (Hossain et al., 2020).

A stronger policy is the sealing of borders to interfere with the movement of people. Blockades eliminate the possibility of importing infectious diseases, but the economic damage is very high because logistics are disrupted. This could also lead to a shortage of resources and vaccines needed for treatment and diagnosis in endemic countries. Indeed, when the omicron strain of COVID-19 was confirmed in South Africa, several countries closed their borders, and the countries were evacuated.

The geographical spread of infectious diseases associated with human migration has been discussed since the plague epidemics of the 14th century (Murray, 2003). Many studies have been conducted on the geographical spread of rabies in Europe and the USA (Bacon, 1985). In the above studies, the geographical spread was mainly based on diffusion; however, in modern times, airplanes are mainly used to travel between large cities. Therefore, attention has been drawn to spread based on airline networks, using the time of arrival, that is, the time from the start of an epidemic to the arrival of the infectious disease in each country, as an indicator (Colizza, Barrat, Barthélemy, & Vespignani, 2005; Gautreau, Barrat, & Barthélemy, 2007; Hwang et al., 2012). Brockmann & Helbing and Kuo & Chiu used the effective distance, a metric based on the flow of people, to assess arrival time (Brockmann & Helbing, 2013; Kuo & Chiu, 2021). Similarly, Jamieson-Lane & Brasius used a branching process to describe the transmission process of infectious diseases and computed arrival time (Jamieson-Lane & Blasius, 2020). Although it has been suggested that the increase in the number of infected cases in an endemic country is closely related to the arrival time (Poletto et al., 2014; Tomba & Wallinga, 2008), the impact of implementing health policies in endemic countries and strengthening quarantine in disease-free countries has not been directly compared because of the different objectives of the interventions.

In this study, we constructed a hybrid model that describes the dynamics of infection in an endemic country using differential equations and the movement of people using stochastic processes. The model thus constructed is then used to compare the effects of how aid to the endemic country affects arrival time and how quarantine delays arrival time, based on simulations.

The remainder of this paper is organized as follows. The Materials and Methods section introduces the SIR and SEIR models using deterministic ordinary differential equations (ODEs) and their implementation in a health policy model. In general, the transmission of infectious diseases exhibits stochastic behavior. To implement this randomness, we introduce a model based on random ordinary differential equations (RODEs), which are differential equations with stochastic processes in their vector field functions. Furthermore, a survival time function for human migration is introduced to calculate the arrival time. In the Results section, an analytical description of the arrival time based on the SIR model is provided. The impact of a decrease in the transmission rate on arrival time is also assessed. The second example simulates the SEIR model to investigate the relationship between medical interventions and the arrival time of infected cases. In the third example, the SEIR model described by RODEs is used to investigate the effect of medical intervention in an endemic country and the strengthening of quarantine on arrival time, to estimate the number of infected cases in the endemic country. In the Discussion section, based on the results of the above simulations, we summarize the results of interventions for different targets, namely, testing and isolation in endemic countries and quarantine in disease-free countries, along with a discussion on the desired medical policy and interventions in the future.

2. Material and methods

2.1. SIR model

The SIR model introduced by Kermack and McKendrick in 1927 describes the transmission of infectious diseases (Kermack & MacKendrick, 1927). The model describes the interaction of three compartments: susceptible, infected, and recovered/removed, and is expressed in the following form:

$$\frac{\mathrm{d}S}{\mathrm{d}t} = -\beta \frac{S(t)}{N} I(t) \tag{1}$$

$$\frac{dI}{dt} = \beta \frac{S(t)}{N} I(t) - \gamma I(t) \tag{2}$$

$$\frac{dR}{dt} = \gamma I(t), \tag{3}$$

where β is the transmission rate; γ is the recovery rate; and $N = S + I + R$. Measures, such as wearing masks and physical distancing, are assumed to reduce the transmission rate. If the effect of the measures is $\varepsilon \in [0, 1]$, the transmission rate can be described as $(1 - \varepsilon) \times \beta$ to obtain the dynamics of infectious diseases when physical distancing is increased.

2.2. SEIR model

Infectious diseases, including COVID-19, have an incubation period. The SEIR model is implemented in the SIR model by assuming that cases are exposed during the incubation period (Diekmann, Heesterbeek, & Britton, 2013; Vynnycky & White, 2010). Assuming an incubation period of $1/\sigma$, the SEIR model is given by

$$\frac{dS}{dt} = -\beta \frac{S(t)}{N} I(t) \tag{4}$$

$$\frac{dE}{dt} = \beta \frac{S(t)}{N} I(t) - \sigma E(t) \tag{5}$$

$$\frac{dI}{dt} = \sigma E(t) - \gamma I(t) \tag{6}$$

$$\frac{dR}{dt} = \gamma I(t), \tag{7}$$

where $N = S + E + I + R$. Consider a scenario in which an infected person is diagnosed by PCR testing and placed in isolation. If the sensitivities of the PCR test are ρ_E and ρ_I for exposed and infected individuals, respectively, the flow from infection to recovery/isolation can be described as shown in the following diagram (Fig. 1).

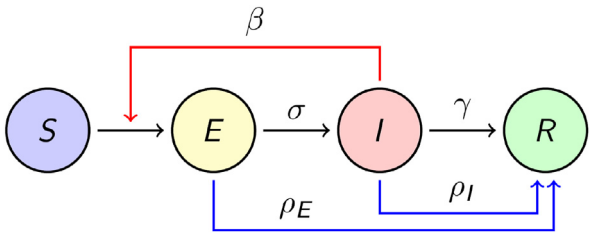

Fig. 1. Local dynamics in an outbreak country C_0 described by the SEIR model with an isolation effect.

It is impractical to perform PCR testing on all individuals. Therefore, in practice, PCR testing is recommended in cases of suspected infection through contact tracing, etc., and if the test is positive, the patient is placed in isolation. Assuming the proportion of identified exposed and infected individuals by τ_E and τ_I, respectively, the model with targeted PCR testing can be described using the following equations:

$$\frac{dS}{dt} = -\beta \frac{S(t)}{N} I(t) \tag{8}$$

$$\frac{dE}{dt} = \beta \frac{S(t)}{N} I(t) - \sigma E(t) - \rho_E \tau_E E(t) \tag{9}$$

$$\frac{dI}{dt} = \sigma E(t) - \gamma I(t) - \rho_I \tau_I I(t) \tag{10}$$

$$\frac{dR}{dt} = \gamma I(t) + \rho_E \tau_E E(t) + \rho_I \tau_I I(t). \tag{11}$$

2.3. Modeling by RODEs

The SIR and SEIR models are deterministic, and parameters such as β, σ, and γ are assumed to be constant. Although deterministic models are useful, including their application in dynamical systems, the spread of infection shows stochastic behavior and the epidemic curve alone shows more complex behavior in practice. Therefore, stochastic processes, continuous-time Markov chain models, and stochastic differential equations (SDEs) have been introduced and studied (Allen, 2017; Bailey, 1964; Capasso & Bakstein, 2015; Daley & Gani, 1999). Allen also included the interactions of individual compartments and introduced uncertainty into the model (Allen, 2007).

SDEs are well-known for their use in fields such as economics, finance, biology, medicine, and engineering (Capasso & Bakstein, 2015; Caraballo & Han, 2016; Gerstner & Kloeden, 2012). SDEs are useful; however, undesirable phenomena, such as negative parameters or diffuse values can occur in the simulations. Furthermore, cases in which the noise process is not normally distributed have been observed (d'Onofrio, 2013). Therefore, in this study, modeling using RODEs is considered.

RODEs are differential equations with stochastic processes in their vector-field functions. RODEs are considered pathwise as ODEs and have been used in various fields, such as biology, medicine, and population dynamics (Bunke, 1972; Han & Kloeden, 2017; Neckel & Rupp, 2013). They also play an important role in random dynamical systems (Arnold, 1997) but have long been overshadowed by SDEs. In general, RODEs can be described as follows:

$$\frac{\mathrm{d}x}{\mathrm{d}t} = f(x, Z_t),$$

where Z_t denotes a stochastic process. Regular noise can be implemented in RODE, including continuous noise processes, such as Brownian motion and fractional Brownian motion as well as processes with jumps, such as the Poisson process and compound Poisson process. The SEIR model was described and simulated in this study using RODE.

If we include the effect of migration in the SEIR model, we obtain the following equation:

$$\frac{\mathrm{d}S}{\mathrm{d}t} = \mu N(t) - \beta \frac{S(t)}{N} I(t) - \mu S(t) \tag{12}$$

$$\frac{\mathrm{d}E}{\mathrm{d}t} = \beta \frac{S(t)}{N} I(t) - \sigma E(t) - \mu E(t) \tag{13}$$

$$\frac{\mathrm{d}I}{\mathrm{d}t} = \sigma E(t) - \gamma I(t) - \mu I(t) \tag{14}$$

$$\frac{\mathrm{d}R}{\mathrm{d}t} = \gamma I(t) - \mu R(t), \tag{15}$$

where μ is a parameter corresponding to people's movement. It is known that the number of people leaving the country is generally not the same as the number of people entering it and that the number of people traveling decreases during infectious disease outbreaks due to travel restrictions and self-restraint. Although implementing a reduction in human mobility would be more realistic, it is difficult to predict changes in human movements, and this study did not assume a reduction in the number of travelers. On the other hand, it is not realistic to set μ as a constant, so it is described as a stochastic process using (16) below. In addition, the transmission rate is strongly influenced by policies, such as teleworking and school closures. Therefore, β is also described by a stochastic process (17):

$$\mu(Z_t) \coloneqq \mu_0 \left(1 - \frac{2\nu_\mu}{\pi} \arctan Z_t\right), \tag{16}$$

$$\beta(Z_t) \coloneqq \beta_0 \left(1 - 2\nu_\beta \frac{Z_t}{1 + Z_t^2}\right). \tag{17}$$

Using the above equations (16) and (17), $\mu \in [\mu_0(1-\nu_\mu), \mu_0(1+\nu_\mu)]$ and $\beta \in [\beta_0(1-\nu_\beta), \beta_0(1+\nu_\beta)]$, if we set $\mu_0(1-\nu_\mu)$ and $\beta_0(1-\nu_\beta) > 0$, stochastic processes with non-negative finite width can be generated.

Because RODEs include stochastic processes, the numerical methods for deterministic models do not maintain the same order of convergence. Therefore, numerical methods for RODEs have been developed in recent years. For more details on RODEs and the numerical methods for RODEs, see (Asai, Cheng, & Han, 2023; Asai & Kloeden, 2013, 2019; Han & Kloeden, 2017) and the references therein.

2.4. Migration and arrival time

To model the movement of people in a day, we consider the number of infected individuals I_n on day n as a discrete value instead of a continuous value $I(t)$. For simplicity, consider the movement of people between two countries: the endemic country C_0 and the disease-free country C_i.

If M_i people move from C_0 to C_i per day, the probability μ_i that each person moves from C_0 to C_i is given by $\mu_i = M_i/N$, where N is the population of C_0. Define $Surv(n-1)$ as the probability that no infected person reaches C_i on day $(n-1)$. Then, $Surv(n)$, the probability of not reaching day n, is given by

$$Surv(n) = Surv(n-1) \times (1-\mu_i)^{I_n}.$$

This implies that the probability that no infected person reaches C_i by day n from the start of the epidemic is:

$$Surv(n) = (1-\mu_i)^{I_1} \times \cdots \times (1-\mu_i)^{I_n} = \prod_{j=1}^{n} (1-\mu_i)^{I_j}. \tag{18}$$

Suppose that the day n^* satisfies $Surv(n^*) = 1/2$. Then, the probability that at least one infected individual arrives at C_i becomes $1 - Surv(n) \geq 1/2$ for $n \geq n^*$, i.e., the probability of importation, is 1/2 or more after the day n^*. Using this relationship, the number of infected people in the endemic country, infection-related parameters, human flow μ_i, and arrival time n can be described using a single equation. If the expression for I_{n^*} is complex, as in this study, an analytical expression for n^* cannot be obtained and must be computed numerically.

An alternative idea for estimating the arrival time is to use a geometric distribution. The geometric distribution is given by the probability of first success on the $(n+1)$-th attempt after n attempts and is a useful probability distribution for considering the arrival of infected cases. The geometric distribution and the cumulative number of infected cases in the epidemic country C_0 can be used to calculate the expected value of the number of cases that will arrive. The geometric distribution might be suitable in small epidemics. This study, however, focuses on the arrival time, i.e., the days when an infectious disease is expected to be imported, and the model was formulated using a form of survival time.

In the next section, the SIR, SEIR, and RODE models are used to estimate the number of infected cases in the endemic country C_0 and to obtain the arrival time. In general, the probability of migration is expected to be different for susceptible and infected populations, but in this study, it is assumed that all individuals have the same μ_i probability of migration.

The same reasoning can be applied to cases in which there are multiple destinations. Suppose that there is a movement of people from C_0 to m countries and $\mu = \sum_{i=1}^{m} \mu_i$ (Fig. 2). Then, in the scenario of migration to C_i, the total number of people migrating from C_0 is calculated, and $\mu_i \times N$ is subsequently extracted. The extracted numbers E and I are the numbers of exposed and infected individuals migrating from C_0 to C_i.

Assuming that the quarantine measure is a PCR test, it is conceivable that the effectiveness of quarantine depends on ρ_E and ρ_I introduced in Section 2.2. Indeed, if $\mu_i \times E$ and $\mu_i \times I$ have moved from C_0 to C_i, the PCR test is positive with probabilities of ρ_E and ρ_I, respectively. Conversely, it will be negative with probabilities $(1-\rho_E)$ and $(1-\rho_I)$ for movement in the opposite direction (Fig. 3). The higher the sensitivity of the PCR test, the higher the probability of catching an infected person in quarantine. On the other hand, if ρ_E and ρ_I are low, more infected people are allowed to enter C_i, which may lead to the spread of infection within C_i.

In general, arrival time refers to the time between the outbreak of an epidemic in C_0 and the arrival of infected cases in a disease-free country C_i, and cases stopped at airport quarantine are also counted as imported cases. Conversely, a major

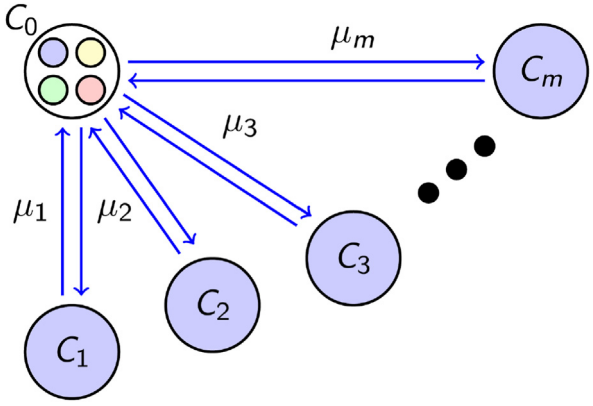

Fig. 2. Migration from an outbreak country C_0 to disease-free countries $C_i (i = 1, \ldots, m)$.

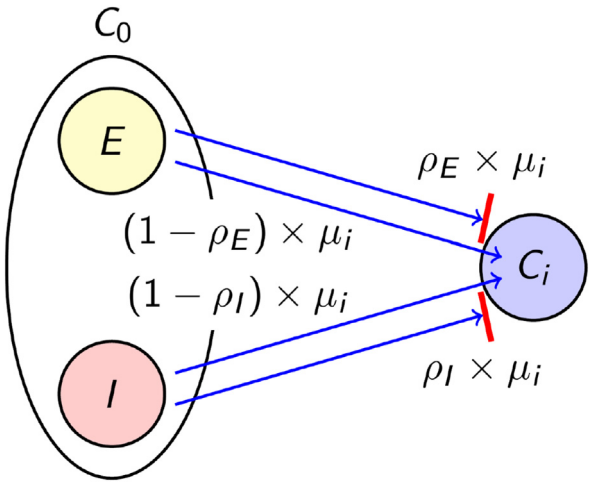

Fig. 3. Effect of quarantine measure at disease-free country C_i.

concern in disease-free countries is that imported cases may lead to community-acquired infections and increase the number of infected cases in their countries. In this study, arrival was defined as a situation in which a case slips through quarantine and leads to community-acquired infection or an epidemic in disease-free countries.

This study used hypothetical data for a movement of people μ_i, but in practice, human flows are estimated from airline network data (Brockmann & Helbing, 2013; Colizza et al., 2005; Kuo & Chiu, 2021). The International Air Transport Association (The International Air Transport Association, 2023) provides a complete data set of the world's airline network, and the structure and topology of the network have been intensively studied in recent years (Barrat, Barthélemy, Pastor-Satorras, & Vespignani, 2004). The IATA data can be applied to more practical problems, such as the impact of the changing network structure on the global spread of infectious diseases. Visualization of the airline networks and the spread of infectious diseases can be found on the website by Brockmann (Brockmann Lab, 2023).

3. Results

3.1. SIR model

During the early stages of an epidemic, it can be assumed that $S \approx N$. Then, Equation (2) becomes

$$\frac{\mathrm{d}I}{\mathrm{d}t} = \beta I(t) - \gamma I(t),$$

and $I(t) = I_0 e^{(\beta-\gamma)t}$, where $I(0) = I_0$ is the initial value. Because this study assumes a scenario in which the infection spreads, $\beta > \gamma$. The above equation is substituted into (18) to calculate the arrival time n^*, which is the threshold for importation with 1/2 possibility. By solving this equation with respect to n^*, we obtain

$$\begin{aligned} n^* &= \frac{1}{(\beta-\gamma)}\log\left(1+\left(1-e^{-(\beta-\gamma)}\right)\frac{\log\frac{1}{2}}{I_0\log(1-\mu)}\right), \\ &= \frac{1}{\gamma(\mathcal{R}_0-1)}\log\left(1+\left(1-e^{-\gamma(\mathcal{R}_0-1)}\right)\frac{\log\frac{1}{2}}{I_0\log(1-\mu)}\right), \end{aligned} \tag{19}$$

where $\sum_{j=1}^{n^*} e^{(\beta-\gamma)j} = (e^{n^*(\beta-\gamma)}-1)/(1-e^{-(\beta-\gamma)})$ and $\mathcal{R}_0$ is the basic reproduction number given by β/γ.

Wearing a mask and physical distancing can reduce human contact. Assuming that the effect is $\varepsilon \in [0,1]$, the transmission rate is reduced to $(1-\varepsilon)\times\beta$, as described in Section 2.1. By substituting this into (19), the arrival time under the health policy can be calculated. When $(\beta-\gamma)$ is large, $e^{-(\beta-\gamma)}$ approaches zero, and thus, $1/(\beta-\gamma)$ is used to determine n^*. If this term is given by $1/((1-\varepsilon)\times\beta-\gamma)$, then n^* becomes larger, implying that the arrival time is delayed.

Fig. 4 shows the results of the simulation with the ε effect of the health policy set to 0.1 and 0.2. In this simulation, the initial value was $I_0 = 1$ and the parameters were set to $\beta = 0.2$, $\gamma = 0.07$, $N = 1\times10^7$ and $10^1/N \le \mu \le 10^3/N$.

Simulations using the SIR model confirmed that the values obtained with (19) and the results obtained with 1,000 simulations were in good agreement. It was also confirmed that lowering the transmission rate to $\beta \times 0.9$ and $\beta \times 0.8$ reduced the number of infected individuals within C_0, resulting in a slower arrival time. In fact, the arrival time for a country with 100 travelers from C_0 per day was 33 days when the transmission rate was β but 44 days when $\beta \times 0.8$, indicating that a 20% reduction in the number of new infections leads to an 11-day delay. Similarly, a reduction in the number of people traveling to the country led to a corresponding delay in arrival time. When the transmission rate was β, it was found that in countries with 100 travelers per day, the arrival time was 33 days, while in countries with 10 travelers per day, the delay was 50 days (Table 1).

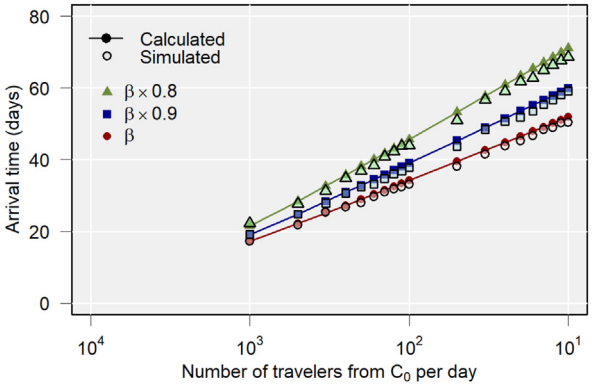

Fig. 4. Estimated arrival time from C_0 based on SIR model.

Table 1
Transmission rate and arrival time calculated by (19) and by simulation.

Transmission rate	Number of travelers from C_0 per day					
	1,000		100		10	
	Calc.	Sim.	Calc.	Sim.	Calc.	Sim.
β	17	17	34	33	52	50
$\beta \times 0.9$	19	19	39	38	60	59
$\beta \times 0.8$	22	22	46	44	71	69

3.2. SEIR model

Similar to Section 3.1, we assume $S \approx N$ and $\beta > \gamma$. Then, (9) and (10) become:

$$\frac{dE}{dt} = \beta I(t) - \sigma E(t) - \rho_E \tau_E E(t)$$
$$\frac{dI}{dt} = \sigma E(t) - \gamma I(t) - \rho_I \tau_I I(t).$$

Analytical solutions to this set of differential equations were obtained using the Laplace transformation (Schiff, 1999).

$$\mathcal{L}\left[\frac{dE}{dt} + (\sigma + \rho_E \tau_E)E(t) - \beta I(t)\right] = 0$$
$$\mathcal{L}\left[\frac{dI}{dt} + (\gamma + \rho_I \tau_I)I(t) - \sigma E(t)\right] = 0$$

By substituting $\tilde{E}(s) = \mathcal{L}[E(s)]$ and $\tilde{I}(s) = \mathcal{L}[I(s)]$, we obtain the following equation:

$$\begin{pmatrix} s + (\sigma + \rho_E \tau_E) & -\beta \\ -\sigma & s + (\gamma + \rho_I \tau_I) \end{pmatrix} \begin{pmatrix} \tilde{E}(s) \\ \tilde{I}(s) \end{pmatrix} = \begin{pmatrix} E_0 \\ I_0 \end{pmatrix}.$$

This leads

$$\tilde{E}(s) = \frac{(s + (\gamma + \rho_I\tau_I))E_0 + \beta I_0}{(s + (\sigma + \rho_E\tau_E))(s + (\gamma + \rho_I\tau_I)) - \beta\sigma}$$
$$\tilde{I}(s) = \frac{\sigma E_0 + (s + (\sigma + \rho_E\tau_E))I_0}{(s + (\sigma + \rho_E\tau_E))(s + (\gamma + \rho_I\tau_I)) - \beta\sigma},$$

where $(s + (\sigma + \rho_E\tau_E))(s + (\gamma + \rho_I)\tau_I) - \beta\sigma \neq 0$.

The inverse Laplace transformation yields:

$$E(t) = \frac{1}{\sqrt{\Delta}}\left\{\sqrt{\Delta}\,E_0\cosh\sqrt{\Delta}\,t + \left(\beta I_0 + \frac{1}{2}(\gamma' - \sigma')E_0\right)\sinh\sqrt{\Delta}\,t\right\}e^{-\frac{1}{2}(\sigma'+\gamma')t}$$
$$I(t) = \frac{1}{\sqrt{\Delta}}\left\{\sqrt{\Delta}\,I_0\cosh\sqrt{\Delta}\,t + \left(\sigma E_0 + \frac{1}{2}(\sigma' - \gamma')I_0\right)\sinh\sqrt{\Delta}\,t\right\}e^{-\frac{1}{2}(\sigma'+\gamma')t}.$$

For simplicity, we have set $\sigma' = \sigma + \rho_E\tau_E$, $\gamma' = \gamma + \rho_I\tau_I$ and $\Delta = (\sigma' + \gamma')^2/4 - \sigma\beta - \sigma'\gamma'$.

Unlike in the case of the SIR model, $E(t)$ and $I(t)$ have a complex form and cannot be solved explicitly for n^*, as in (19). Therefore, $I(t)$ obtained above was substituted for I_j in (18) to obtain the value of n^* numerically. A simulation was also performed to determine the relationship between the effect of the intervention and arrival time. In this simulation, the initial values were $E_0 = 1$ and $I_0 = 3$, and the parameters were set to $\beta = 0.6$, $\sigma = 0.08$, $\gamma = 0.15$, $\rho_I = 0.8$, and $N = 1 \times 10^7$ and $10^1/N \leq \mu \leq 10^3/N$. In addition, ρ_E was set to zero, and a scenario was assumed in which only infected individuals underwent PCR testing and were isolated if they tested positive. Specifically, two effects were assumed: a case with $\tau_I = 0.05$ as weak intervention and $\tau_I = 0.1$ as strong intervention, i.e., the scenarios in which 5% and 10% of infected individuals were identified, respectively, and the arrival time was calculated (Fig. 5).

Similarly, simulations using the SEIR model showed that the numerically obtained n^* values were in agreement with the actual simulation results. It was also confirmed that the intervention of isolation by PCR testing reduced the number of infections and consequently delayed the time of arrival. In fact, if 100 travelers were expected per day, without PCR testing, infections would be imported within 35 days. On the other hand, with strong intervention, it was found to be 48 days, with an expected delay of 13 days. The relationship between the number of travelers and arrival time is similar to that of the SIR model, with a decrease in the number of travelers leading to a delay in arrival time. For example, in a country with 1,000 travelers per day, infectious diseases are imported in 22 days; in a country with 100 travelers, 48 days; and in a country with 10 travelers, 77 days, that is, a delay of at least 30 days can be expected if the number of travelers is reduced by 1/10 (Table 2).

In the country, where 100 travelers are expected per day from C_0, the arrival time of the infected individual is calculated to be on day 36. Conversely, the arrival time of the exposed individuals was calculated to be 26 days, meaning that they had

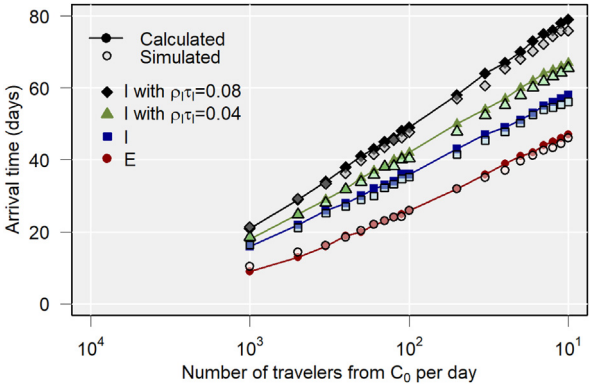

Fig. 5. Estimated arrival time from C_0 based on SEIR model.

Table 2
Transmission rate and arrival time simulated by SEIR model.

Arrived individuals	Number of travelers from C_0 per day					
	1,000		100		10	
	Calc.	Sim.	Calc.	Sim.	Calc.	Sim.
E	9	10	26	26	47	46
I	16	16	36	35	58	57
I with $\rho_I\tau_I = 0.04$	18	19	42	41	67	65
I with $\rho_I\tau_I = 0.08$	21	22	49	48	79	77

already entered the country C_i 10 days earlier. For the country with 1,000 expected travelers, the arrival time was calculated to be nine days, compared to 16 days for the infected individuals.

3.3. Simulation by RODE

Here, we describe the epidemic of infectious diseases in an endemic country C_0 using the model introduced in Section 2.3. The flow of people from the endemic country to disease-free countries was simulated, and the arrival time was calculated.

To generate $\beta(Z_t)$ and $\mu(Z_t)$, first it is necessary to generate Z_t. In this study, the Ornstein-Uhlenbeck process was used for Z_t:

$$dZ_t = (\theta_1 - \theta_2 Z_t)dt + \theta_3 dW_t,$$

where θ_1 is non-negative and θ_2 and θ_3 are positive constants. Substituting Z_t into (16) and (17) provides stochastic processes with finite widths. In fact, for $\beta(Z_t)$ with $\theta_1 = 2$, $\theta_2 = 1$, $\theta_3 = 5$, $\beta_0 = 4 \times 10^{-8}$ and $\nu_\beta = 0.5$, the following example path is obtained as in Panel A of Fig. 6. It is observed that $\beta(Z_t)$ has many values around $\beta_0(1 - \nu_\beta)$ and $\beta_0(1 + \nu_\beta)$. Panel B of Fig. 6 confirms that the switching effect is realized.

For $\mu(Z_t)$, assuming $\theta_1 = 1$, $\theta_2 = 3$, $\theta_3 = 7$, $\mu_0 = 1 \times 10^{-4}$ and $\nu_\mu = 0.5$, the sample path was generated as in Panel A of Fig. 7. As with $\beta(Z_t)$, it was confirmed that a finite-width stochastic process can be generated.

In the following simulation, PCR testing and isolation were assumed as the medical policies. Currently, apps with Bluetooth functionality are used to inform users of contact with an infected person (Min-Allah et al., 2021). Contact tracing by health centers uses interventions, such as identifying potentially infected individuals and encouraging them to undergo PCR testing. However, not all infected individuals are necessarily identified, and there may be infected individuals who do not undergo PCR testing. Therefore, two types of PCR testing were considered: random and targeted. In targeted testing, it is assumed that some of the exposed and infected individuals are identified through contact tracing, and PCR is performed on these individuals, with positive results leading to isolation.

In the following simulation, the parameters and initial values were set to $\sigma = 0.3$, $\gamma = 0.15$, $\rho_E = 0.6$, $\rho_I = 0.8$, $\mu_0 = 2 \times 10^{-4}$, $\nu_\mu = 0.5$, $\beta_0 = 7 \times 10^{-8}$, $\nu_\beta = 0.5$, $E_0 = 5$, $I_0 = 1$, $R_0 = 0$, $S_0 = N - E_0 - I_0 - R_0$, and $N = 1 \times 10^7$, respectively. The results of the simulation using the RODE model are shown in Fig. 8. In particular, the proportion of target cases $\tau = \tau_E = \tau_I$ was set to 0 ~ 35% and the number of infected and recovered cases in the endemic country C_0 was plotted. A targeted proportion of 0%, that is, random testing, peaked at around 60 days, resulting in 8×10^6 and 80% of the population being infected by day 100.

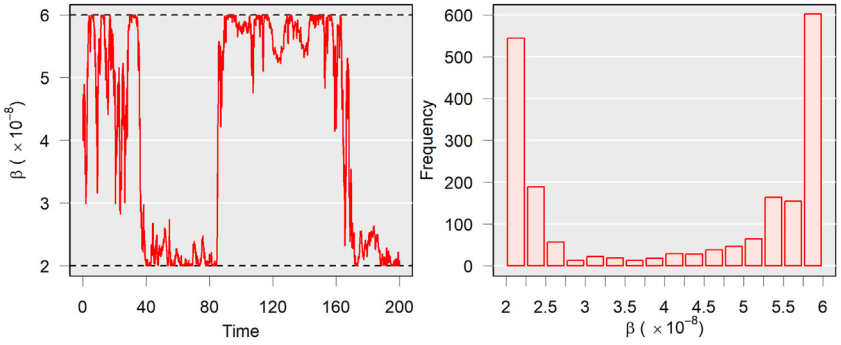

Fig. 6. A sample path of switching noise $\beta(t)$.

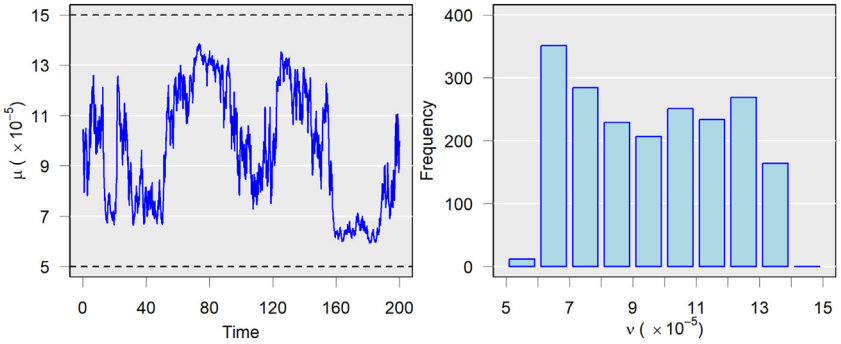

Fig. 7. A sample path of centered noise $\mu(t)$.

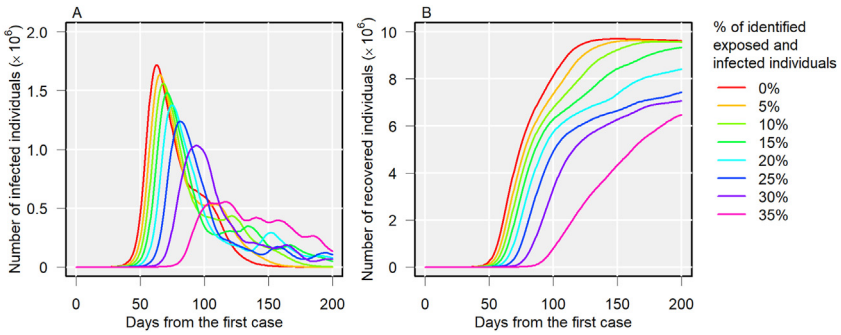

Fig. 8. Number of infected individuals and recovered individuals under different identification rates.

Furthermore, almost the entire population was infected by day 120. The peak in the number of infected people decreased as the proportion of targeted individuals increased, and a rightward shift in the peak was observed. In the scenario where 35% of the infected individuals could be identified, the peak number of infected individuals was 6×10^5 and the total number of infected individuals on day 100 was less than 1×10^6.

PCR tests are widely used but are limited in number and expensive. In this study, the number of available kits per day was set to $N \times \mu_0 \times 2 = 4 \times 10^3$, which is twice the number of travelers per day. Two scenarios were then considered: one in which all the kits were used in the endemic country C_0, and the other in which the disease-free countries C_i used some of them to quarantine travelers from C_0. The number of travelers to disease-free countries per day was 2×10^3, and if a kit of 2×10^3 was used in C_0, PCR tests were performed on all travelers in quarantine. If a kit of 3×10^3 was used in C_0, the scenario corresponded to PCR testing of not all travelers but of 1×10^3 travelers, that is, half of them. In many cases, the epidemic is not widely recognized in its early stages. Therefore, the following simulation assumes that PCR testing begins when $I(t)$ exceeds 100.

Panel A of Fig. 9 shows the relationship between the number of daily travelers from C_0 and arrival time. Here, the number of PCR kits used in C_0 and the number of PCR kits used for those quarantined in C_i were both set to 2×10^3 and it was assumed that PCR tests are performed on all travelers. Similar to the results from the SIR and SEIR models, it was confirmed that a reduction in the number of travelers leads to a delay in the arrival time. The slope of the arrival time with respect to the number of travelers was gentler when the proportion of identified infections was 0, that is, when PCR testing was performed on randomly selected individuals. However, as the identification rate increased, the slope increased, which had a greater effect on delaying the arrival time. Panel B of Fig. 9 evaluates the effect of the number of kits used in C_0 as well as the effect of the identified proportion of infected persons on the arrival time, for countries with 100 travelers from C_0. The results indicate that a delay of 10 days could not be expected when the identified proportion was less than 10%, regardless of whether the number of PCR kits was high or low. However, a delay of more than 60 days could be expected if 30% could be identified. It was also found that increasing the number of PCR kits used in C_0 led to a delay in the arrival time, but not necessarily to a significant effect.

Fig. 10 Panel A shows the cumulative number of infected patients at C_0 on days 60, 80, and 120, and panel B shows the cumulative number of infected patients on day 200. Random testing confirmed that the cumulative number of infected people exceeded 1×10^6 on day 60. This trend was also evident on days 80 and 120, when the number of infected individuals exceeded 5×10^6 and 9×10^6, respectively. On the other hand, when more than 20% of the infections were identified, the number of infections was as low as $1.0 \sim 1.5 \times 10^5$ on day 60, which was also the case on day 80. However, by day 120, the number of infected persons exceeded 6×10^6, and, as shown in panel B, by day 200, the number of infections exceeded 8×10^6. New infections were significantly suppressed when the specified proportion exceeded 30%, and even on day 80, the number of new infections was $2 \sim 5 \times 10^5$. As shown in panel B, if 35% of infected persons could be identified, the number of

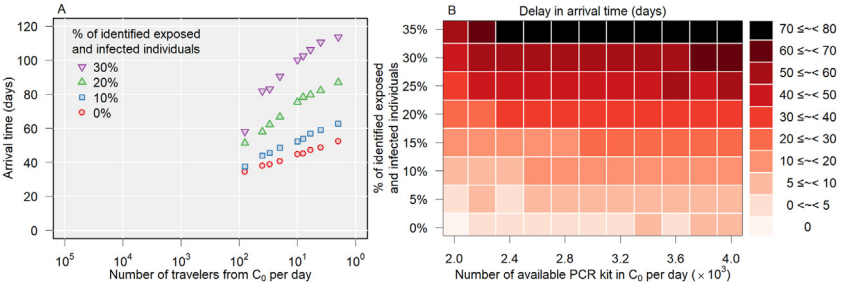

Fig. 9. Relationship between arrival time and the number of travelers from C_0 and the delay of arrival time based on the percentage of the identified exposed and infected individuals and the number of available PCR kits in C_0.

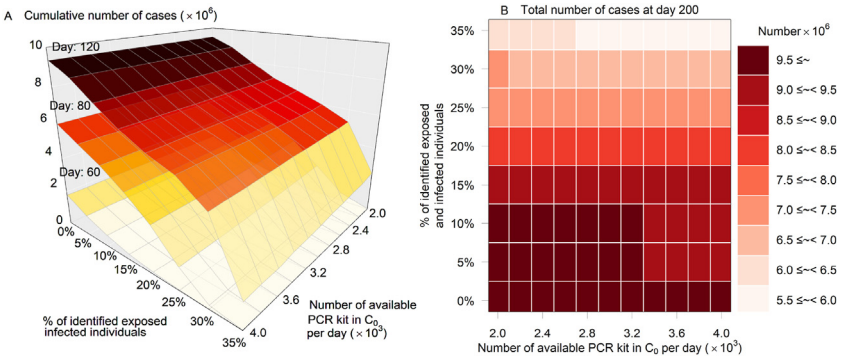

Fig. 10. Cumulative number of cases in C_0 based on the percentage of the identified exposed and infected individuals and the number of available PCR kits in C_0.

infected persons would be approximately 6×10^6 on day 200, and if the number of PCR kits available at C_0 exceeded 2.8×10^3, the simulation results showed that the number of infected persons would be less than 6×10^6.

3.4. Simulation algorithm

In this section, we present a simulation algorithm for the RODE model. The notation in Section 3.3 was used for the parameters. In addition, τ_E and τ_I denote the proportion of identified exposed and infected individuals, respectively, and N_{PCR} denotes the number of available PCR kits per day.

1. Specify parameter values and initial values at $t = t_0$. Set calculation point t_n and the number of steps n with a step size $\Delta_t = (t_n - t_0)/n$.
2. Set $j = 0$.
3. Loop while $j < n$
   - 3-1. Generate stochastic processes $\beta(Z_t)$ and $\mu(Z_t)$ at $t = t_j$.
   - 3-2. Simulate the RODE model and compute the numbers at $t = t_j + \Delta_t$.
   - 3-3. Select $\mu_i \times N$ travelers from the entire population without replacement.
     - 3-3-1. Count the number of E and I among selected travelers and apply the binomial distribution to each of them with ρ_E and ρ_I, respectively.
       - E and I individuals who happen to have a negative result enter C_i (Arrived).
       - E and I with a positive result remain in quarantine (Not arrived).
   - 3-4. Select $(\tau_E E + \tau_I I)$ individuals for PCR testing, without replacement.
     - 3-4-1. Count the number of E and I chosen and apply the binomial distribution to each one with ρ_E and ρ_I, respectively.
       - E and I individuals who happen to have a negative result return to compartments E and I, respectively.
       - E and I that are positive move to compartment R (Isolation).
   - 3-5. $j = j + 1$
4. Stop

Repeat steps 3-3 for $i = 1, \ldots, m$. In steps 3–4, if $(\tau_E E + \tau_I I)$ is greater than the number of assigned PCR kits N_{PCR}, apply the binomial distribution N_{PCR} times and release the remaining individuals.

4. Discussion

In this study, a hybrid model integrating the SIR, SEIR, and RODE models with human migration was constructed. The constructed model was used to investigate the effect of an increase in the number of infected people in the endemic country C_0 on the arrival time in disease-free countries C_i. We also examined the effect of measures to reduce the transmission rate, such as the use of masks and physical distancing as well as the effect of health policies, such as the promotion of isolation by PCR testing, on the arrival time.

In the analysis using the SIR model, arrival time n^* is given by β and γ, the parameters that determine the infection dynamics, and μ_i, the proportion of travelers from C_0 to C_i. The number of infected individuals among travelers was counted by random sampling from C_0, and it was confirmed that the theoretical solution was consistent with the simulation results (Fig. 4, Table 1). Unlike in the SIR model, no analytical expression for n^* could be derived from the SEIR model. However, it was confirmed that the value of n^* obtained numerically was consistent with the simulation results.

As we observed, there is a difference between the arrival time of infected and exposed individuals (Fig. 5). In fact, the arrival time of the exposed individuals was more than seven days earlier than that of infected individuals (Table 2). Exposed

individuals, cases during the incubation period, are often asymptomatic and less likely to be detected in quarantine than infected individuals. When the mutation to the Omicron strain was announced in South Africa, several countries imposed travel restrictions on South Africa. However, some countries that imposed restrictions had already imported Omicron strains before the mutant strain was announced. We believe that the model developed in this study can be used in a real-world setting to discuss how many cases may already be in the country and to quantitatively assess the rationale for imposing or not imposing travel restrictions.

A stochastic process was implemented in the RODE model and was simulated using the SEIR model. In the event of an international epidemic of an infectious disease, strong measures are sometimes taken, such as closing borders to protect one's own country. Although the possibility of importing infectious diseases is greatly reduced, the economic impact of closing borders can lead to problems, such as the depletion of necessary medical resources as well as other problems (Emeto, Alele, & Ilesanmi, 2021; COVID-19 and international mobility and trade, 1060; Timur & Xie, 2021; Wilson, Baker, Blakely, & Eichner, 2021). Therefore, this study considered a scenario in which a limited number of PCR kits are distributed between endemic and disease-free countries. The effectiveness of a scenario in which a large number of PCR kits are distributed to the endemic country for cooperation in infectious disease control was compared with that of a scenario in which PCR testing is expanded in the home country.

The results showed that the greater the number of PCR kits used in C_0, the longer the delay in arrival time, and the lower the cumulative number of infections. This suggests that a longer delay effect can be expected in C_i by distributing more kits to C_0 than quarantining in C_i. Furthermore, the trend of using all PCR kits at C_0 is more effective than distributing them, which becomes more pronounced as the proportion of identified infected individuals increases. However, if the number of infected individuals is difficult to identify and the proportion is 0%, then PCR testing is not expected to be effective for the population in C_0. If a delay of 30 days is required, then an identified proportion of 20% and a PCR kit of at least 2.4×10^3 or an identified proportion of at least 25% would be required. Assistance from disease-free countries could reduce the increase in the number of new infections; however, this alone may not be sufficient to control infections and cannot be expected to provide a sufficient delay. Identifying 25% of cases and encouraging them for testing might be difficult; however, a study by Smith et al. found that 10.9% of individuals who had closed contacts with infected cases would be isolated for the recommended period (Smith et al., 2021). In addition to Bluetooth devices, many contact investigations are carried out by public health departments. Furthermore, people who are not identified as closed contacts but have symptoms may lead to voluntary testing and self-isolation (Centers for Disease Control and, 2019). The performance of smartphones and smartwatches in recent years has been remarkable, and a higher identification rate can be achieved in the future, given the future development of mobile health.

Several studies are underway, including the identification of infected persons through contact tracing (Min-Allah et al., 2021; Vogt, Haire, Selvey, Katelaris, & Kaldor, 2022). Some studies have suggested that more emphasis should be placed on testing capacity and surveillance activities rather than border controls (Emeto et al., 2021). A system for investigating foci of infection using data from self-reporting systems has also been studied and is known to lead to timely self-isolation and emergency testing (Canas et al., 2021). In the present study, simulations were performed assuming PCR testing, but it is also known that increased test sensitivity does not have a significant impact on the control of new infections but depends largely on the frequency of testing and the speed of reporting (Larremore et al., 2021). The development and improvement of technology in health-related infrastructure, including the above-mentioned digital health, is considered important in curbing the international epidemic of infectious diseases.

The SIR and SEIR models were used in this study to describe the transmission dynamics within the epidemic country. They are simple and useful; however, as human contacts are known to follow a contact matrix (Mossong et al., 2008), the age-structured model, which incorporates the population structure, is probably more appropriate. Indeed, when considering human mobility, it is assumed that young and middle-aged people are more mobile than children and the elderly, and that this group has more opportunities to meet others, which may contribute to the transmission of infectious diseases. In addition, staying at home and self-isolation are non-pharmaceutical interventions and are known to control epidemics effectively (Zhang, Wang, Lv, & Pei, 2022). Furthermore, quarantine periods of 10–14 days can prevent the further spread of infectious diseases (Ashcroft, Lehtinen, Angst, Low, & Banhoeffer, 2021; Hossain et al., 2020; Patel, Patel, Fulzele, Mohod, & Chhabra, 2020). More realistic predictions can be achieved by adding models with suitable structures and various medical interventions to the hybrid model framework established in this study.

This study has several limitations. First, the assumption of $S \approx N$ in the SIR and SEIR models is so strong that the impact of this assumption needs to be assessed when making long-term projections. Second, the issue of the distribution of PCR kits was considered, but there are various other medical interventions, such as vaccination campaigns and voluntary curfews, and even PCR testing requires a lot of manpower. In addition, many countries have a quarantine policy of isolating people in hotels for two weeks after they arrive in the country; therefore, it is necessary to compare quarantine measures other than PCR testing. Although the time of arrival and the cumulative number of infected persons were used as outcome measures in this study, it is necessary to determine the medical policy, including economic costs. Third, this study considered a scenario in which there is only one endemic country, and the infection spreads from there. However, community-acquired infections may occur in the country of entry, thereby spreading to other countries. It may be necessary to consider building a more realistic model, for example, by running simulations based on actual data to obtain the parameter values.

5. Conclusions

This study found that if the border is not sealed and the flow of people is maintained, a delay in arrival time can be expected by providing more support to the endemic country and controlling new infections rather than by strengthening quarantine. In contrast, it has also been confirmed that random testing does not lead to the suppression of new infections and cannot be expected to significantly delay arrival time. Techniques are being developed to identify individuals with potential infections through contact tracing and Bluetooth devices. Global cooperation in the use of medical resources and the improvement of digital health infrastructure, including medical care, are factors in the containment of international infectious disease epidemics, and further cooperation and development are expected in the future.

Declaration of competing interest

The authors declare that they have no known competing financial interests or personal relationships that could have appeared to influence the work reported in this paper.

Acknowledgement

YA received funding from the Japan Society for the Promotion of Science (JSPS) KAKENHI (grant numbers 17KT0119, 18K17371, 21K17321, and 21H04595).

References

d'Onofrio, A. (2013). *Bounded Noise in physics, biology, and engineering. Birkhäuser*. New York: Springer Science+Business Media.
Allen, E. (2007). *Modeling with itô stochastic differential equations*. Springer.
Allen, L. J. S. (2017). A primer on stochastic epidemic models: Formulation, numerical simulation, and analysis. *Infect Dis Model, 2*(2), 128–142. https://doi.org/10.1016/j.idm.2017.03.001
Arnold, L. (1997). *Random dynamical systems*. Berlin: Springer-Verlag.
Asai, Y., Cheng, J., & Han, X. (2023). *Dynamics of an SEIR model for infectious diseases in random environments. Mathematical modelling: Theory and application, contemporary mathematics*. AMS (in press).
Asai, Y., & Kloeden, P. E. (2013). Numerical schemes for random ODEs via stochastic differential equations. *Communications in Applied Analysis, 17*(3–4), 511–528.
Asai, Y., & Kloeden, P. E. (2019). Numerical schemes for ordinary delay differential equations with random noise. *Applied Mathematics and Computation, 347*, 306–318. https://doi.org/10.1016/j.amc.2018.11.033
Ashcroft, P., Lehtinen, S., Angst, D. C., Low, N., & Banhoeffer, S. (2021). Quantifying the impact of quarantine duration on COVID-19 transmission. *Elife, 10*, Article e63704. https://doi.org/10.7554/eLife.63704, 2021.
Bacon, P. J. (1985). *Population dynamics of rabies in wildlife*. Academic Press.
Bailey, N. T. J. (1964). *The elements of stochastic proceses with applications to the natural sciences*. John Wiley & Sons, Inc.
Barrat, A., Barthélemy, M., Pastor-Satorras, R., & Vespignani, A. (2004). The architecture of complex weighted networks. *Proceedings of the National Academy of Sciences of the U S A, 101*(11), 3747–3752. https://doi.org/10.1073/pnas.0400087101
Brockmann Lab - research on complex systems. Retrieved from https://rocs.hu-berlin.de/visualizations/. (Accessed 11 April 2023).
Brockmann, D., & Helbing, D. (2013). The hidden geometry of complex network-driven contagion phenomena. *Science, 13;342*(6164), 1337–1342. https://doi.org/10.1126/science.1245200
Brümmer, L. E., Katzenschlager, S., Gaeddert, M., Erdmann, C., Schmitz, S., Bota, M., et al. (2021). Accuracy of novel antigen rapid diagnostics for SARS-CoV-2: A living systematic review and meta-analysis. *PLoS Medicine, 12*(8), Article e1003735. https://doi.org/10.1371/journal.pmed.1003735, 18.
Bunke, H. (1972). *Gewöhnliche Differentialgleichungen mit zufälligen Parametern*. Berlin: Akademie-Verlag.
Canas, L. S., Sudre, C. H., Capdevila Pujol, J., Polidori, L., Murray, B., Molteni, E., et al. (2021). Early detection of COVID-19 in the UK using self-reported symptoms: A large-scale, prospective, epidemiological surveillance study. *Lancet Digit Health, 3*(9), e587–e598. https://doi.org/10.1016/S2589-7500(21)00131-X
Capasso, V., & Bakstein, D. (2015). *An introduction to continuous-time stochastic processes theory, models, and applications to finance, biology, and medicine* (3rd ed.). New York: Springer Science+Business Media. Birkhäuser.
Caraballo, T., & Han, X. (2016). *Applied nonautonomous and random dynamical systems applied dynamical systems*. Springer Briefs in Mathematics.
Centers for disease control and prevention isolation and precautions for people with COVID-19. Retrieved from https://www.cdc.gov/coronavirus/2019-ncov/your-health/isolation.html. (Accessed 11 April 2023).
Chu, D. K., Akl, E. A., Duda, S., Solo, K., Yaacoub, S., Schünemann, H. J., & COVID-19 Systematic Urgent Review Group Effort (SURGE) study authors. (2020). Physical distancing, face masks, and eye protection to prevent person-to-person transmission of SARS-CoV-2 and COVID-19: A systematic review and meta-analysis. *Lancet, 27*(10242), 1973–1987. https://doi.org/10.1016/S0140-6736(20)31142-9, 395.
Colizza, V., Barrat, A., Barthélemy, M., & Vespignani, A. (2005). The role of the airpline transportation network in the prediction and predictability of global epidemics. *Proceedings of the National Academy of Sciences of the U S A, 14;103*(7), 2015–2020. https://doi.org/10.1073/pnas.0510525103
COVID-19, international mobility and trade in services: The road to recovery. Retrieved from https://read.oecd-ilibrary.org/view/?ref=1060_1060132-r39k8it7q7&title=COVID-19-international-mobility-and-trade-in-services-The-road-to-recovery. (Accessed 25 January 2023).
Daley, D. J., & Gani, J. (1999). *Epidemic modelling: An introduction*. Cambridge University Press.
Diekmann, O., Heesterbeek, H., & Britton, T. (2013). *Mathematical tools for understanding infectious disease dynamics*. Princeton University Press.
Emeto, T. I., Alele, F. O., & Ilesanmi, O. S. (2021). Evaluation of the effect of border closure on COVID-19 incidence rates across nine african countries: An interrupted time series study. *Transactions of the Royal Society of Tropical Medicine and Hygiene, 115*, 1174–1183. https://doi.org/10.1093/trstmh/trab033
Gautreau, A., Barrat, A., & Barthélemy. (2007). Arrival time statistics in global disease spread. *Journal of Statistical Mechanics: Theory and Experiment*. https://doi.org/10.1088/1742-5468/2007/09/L09001. L09001.
Gerstner, T., & Kloeden, P. E. (2012). Recent developments in computational finance: Foundations, algorithms, and applications. In T. Gerstner, & P. E. Kloeden (Eds.), *Interdisciplinary mathematical sciences* (Vol. 14). World Scientific.
Han, X., & Kloeden, P. E. (2017). *Random ordinary differential equations and their numerical solution*. Singapore: Springer-Verlag.
Hossain, M. P., Junus, A., Zhu, X., Jia, P., Wen, T. H., Pfeiffer, D., et al. (2020). The effects of border control and quarantine measures on the spread of COVID-19. *Epidemics, 32*, Article 100397. https://doi.org/10.1016/j.epidem.2020
Hwang, G. M., Mahoney, P. J., James, J. H., Lin, G. C., Berro, A. D., Keybl, M. A., et al. (2012). A model-based tool to predict the propagation of infectious diseases via airports. *Travel Medicine and Infectious Disease, 10*(1), 32–42. https://doi.org/10.1016/j.tmaid.2011.12.003

Jamieson-Lane, A., & Blasius, B. (2020). Calculation of epidemic arrival time distribution using branching processes. *Physical Review E - Statistical Physics, Plasmas, Fluids, and Related Interdisciplinary Topics, 102*(4–1), Article 042301. https://doi.org/10.1103/PhysRevE.102.042301
Kermack, W. O., & McKendrick, A. G. (1927). A contribution to the mathematical theory of epidemics. *Proceedings of the Royal Society of London, 115*, 700–721.
Kuo, P. F., & Chiu, C. S. (2021). Airline transportation and arrival time of international disease spread: A case study of covid-19. *PLoS One, 19;16*(8), Article e0256398. https://doi.org/10.1371/journal.pone.0256398
Larremore, D. B., Wilder, B., Lester, E., Shehata, S., Burke, J. M., Hay, J. A., et al. (2021). Test sensitivity is secondary to frequency and turnaround time for COVID-19 screening. *Science Advances, 1;7*(1), Article eabd5393. https://doi.org/10.1126/sciadv.abd5393
Min-Allah, N., Alahmed, B. A., Albreek, E. M., Alghamdi, L. S., Alawad, D. A., Alharbi, A. S., et al. (2021). A survey of COVID-19 contact-tracing apps. *Computers in Biology and Medicine, 137*, Article 104787. https://doi.org/10.1016/j.compbiomed.2021.104787
Mina, M. J., & Andersen, K. G. (2021). COVID-19 testing: One size does not fit all. *Science, 8;371*(6525), 126–127. https://doi.org/10.1126/science.abe9187
Mossong, J., Hens, N., Jit, M., Beutels, P., Auranen, K., Mikolajczyk, R., et al. (2008). Social contacts and mixing patterns relevant to the spread of infectious diseases. *PLoS Medicine, 5*(3), e74. https://doi.org/10.1371/journal.pmed.0050074
Murray, J. D. (2003). *Mathematical biology II: Spatial models and biomedical applications* (3rd ed.). New York: Springer.
Neckel, T., & Rupp, F. (2013). *Random differential equations in scientific computing*. Versita, De Gruyter Publishing.
Patel, A., Patel, S., Fulzele, P., Mohod, S., & Chhabra, K. G. (2020). Quarantine an effective mode for control of the spread of COVID19? A review. *Family Med Prim Care, 25;9*(8), 3867–3871. https://doi.org/10.4103/jfmpc.jfmpc_785_20
Poletto, C., Gomes, M. F., Pastore, y, Piontti, A., Rossi, L., Bioglio, L., et al. (2014). Assessing the impact of travel restrictions on international spread of the 2014 West African Ebola epidemic. *Euro Surveillance, 23;19*(42), Article 20936. https://doi.org/10.2807/1560-7917.es2014.19.42.20936
Rosella, L. C., Agrawal, A., Gans, J., Goldfarb, A., Sennik, S., & Stein, J. (2022). Large-scale implementation of rapid antigen testing system for COVID-19 in workplaces. *Science Advances, 25;8*(8), Article eabm3608. https://doi.org/10.1126/sciadv.abm3608
Schiff, J. L. (1999). *The Laplace transform theory and applications*. New York: Springer-Verlag.
Smith, L. E., Potts, H. W. W., Amlôt, R., Fear, N. T., Michie, S., & Rubin, G. J. (2021). Adherence to the test, trace, and isolate system in the UK: Results from 37 nationally representative surveys. *BMJ, 378*, Article o2008. https://doi.org/10.1136/bmj.o2008
Talic, S., Shah, S., Wild, H., Gasevic, D., Maharaj, A., Ademi, Z., et al. (2021). Effectiveness of public health measures in reducing the incidence of covid-19, SARS-CoV-2 transmission, and covid-19 mortality:systematic review and meta-analysis. *BMJ, 17*(375), Article e068302. https://doi.org/10.1136/bmj-2021-068302
The International air Transport association.. Retrieved from. https://www.iata.org/. (Accessed 11 April 2023).
Timur, L., & Xie, Y. (2021). Is border closure effective in containing COVID-19? *Travel Medicine and Infectious Disease, 44*, Article 102137. https://doi.org/10.1016/j.tmaid.2021.102137
Tomba, G. S., & Wallinga, J. (2008). A simple explanation for the low impact of border control as a countermeasure to the spread of an infectious disease. *Mathematical Biosciences, 214*(1–2), 70–72. https://doi.org/10.1016/j.mbs.2008.02.009
Vogt, F., Haire, B., Selvey, L., Katelaris, A. L., & Kaldor, J. (2022). Effectiveness evaluation of digital contact tracing for COVID-19 in New South Wales, Australia. *The Lancet Public Health, 7*(3), e250–e258. https://doi.org/10.1016/S2468-2667(22)00010-X
Vynnycky, E., & White, R. G. (2010). *An introduction to infectious disease modelling*. Oxford University Press.
Wilson, N., Baker, M. G., Blakely, T., & Eichner, M. (2021). Estimating the impact of control measures to prevent outbreaks of COVID-19 associated with air travel into a COVID-19-free country. *Scientific Reports, 24;11*(1), Article 10766. https://doi.org/10.1038/s41598-021-89807-y
World health organization Coronavirus (COVID-19) dashboard. Retrieved from https://covid19.who.int/. (Accessed 5 February 2023).
Zhang, R., Wang, Y., Lv, Z., & Pei, S. (2022). Evaluating the impact of stay-at-home and quarantine measures on COVID-19 spread. *BMC Infectious Diseases, 22*(1), 648. https://doi.org/10.1186/s12879-022-07636-4